Unravelling the structural chemistry of the colouration mechanism in lobster shell. Erratum

Naomi E. Chayen,[a] Michele Cianci,[b] J. Günter Grossmann,[b] Jarjis Habash,[c] John R. Helliwell,[c]* Gwen A. Nneji,[a] James Raftery,[c] Pierre J. Rizkallah[b] and Peter F. Zagalsky[d]

[a]Imperial College, London SW7 2AZ, England, [b]CCLRC Daresbury Laboratory, Warrington WA4 4AD, England, [c]Department of Chemistry, University of Manchester M13 9PL, England, and [d]Royal Holloway and Bedford New College, Egham, Surrey, England. Correspondence e-mail: john.helliwell@man.ac.uk

A corrected version of Fig. 4 from the paper by Chayen *et al.* [(2003), *Acta Cryst.* D**59**, 2072–2082] is given.

Fig. 4 in the article by Chayen *et al.* (2003) was labelled incorrectly along the *x* axis. A corrected version of this figure is given below.

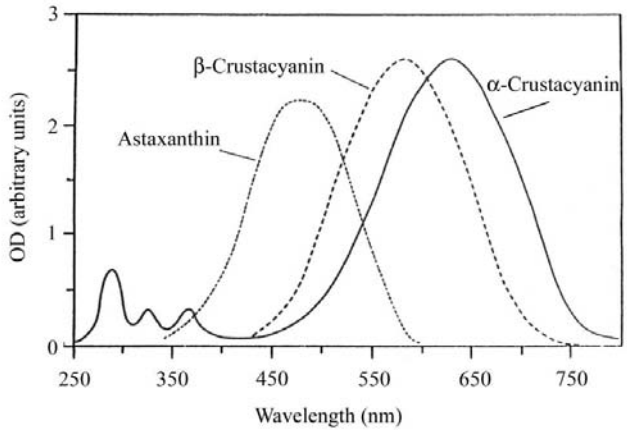

Figure 4
Absorption spectra: astaxanthin in hexane, β-crustacyanin, α-crustacyanin.

References

Chayen, N. E., Cianci, M., Grossmann, J. G., Habash, J., Helliwell, J. R., Nneji, G. A., Raftery, J., Rizkallah, P. J. & Zagalsky, P. F. (2003). *Acta Cryst.* D**59**, 2072–2082.

 © 2005 International Union of Crystallography doi:10.1107/S0907444905019621

Acta Crystallographica Section D
Biological Crystallography
ISSN 0907-4449

Unravelling the structural chemistry of the colouration mechanism in lobster shell

Naomi E. Chayen,[a] Michele Cianci,[b] J. Günter Grossmann,[b] Jarjis Habash,[c] John R. Helliwell,[c]* Gwen A. Nneji,[a] James Raftery,[c] Pierre J. Rizkallah[b] and Peter F. Zagalsky[d]

[a]Imperial College, London SW7 2AZ, England, [b]CCLRC Daresbury Laboratory, Warrington WA4 4AD, England, [c]Department of Chemistry, University of Manchester M13 9PL, England, and [d]Royal Holloway and Bedford New College, Egham, Surrey, England

Correspondence e-mail: john.helliwell@man.ac.uk

Received 2 May 2003
Accepted 10 November 2003

Biochemistry, biological crystallography, spectroscopy, solution X-ray scattering and microscopy have been applied to study the molecular basis of the colouration in lobster shell. This article presents a review of progress concentrating on recent results but set in the context of more than 50 years of work. The blue colouration of the carapace of the lobster *Homarus gammarus* is provided by a multimolecular carotenoprotein, α-crustacyanin. The complex is a 16-mer of five different subunits each binding the carotenoid, astaxanthin (AXT). A breakthrough in the structural studies came from the determination of the structure of β-crustacyanin (protein subunits A1 with A3 with two shared bound astaxanthins). This was solved by molecular replacement using apocrustacyanin A1 as the search motif. A molecular movie has now been calculated by linear interpolation based on these two 'end-point' protein structures, *i.e.* apocrustacyanin A1 and A1 associated with the two astaxanthins in β-crustacyanin, and is presented with this paper. This movie highlights the structural changes forced upon the carotenoid on complexation. In contrast, the protein-binding site remains relatively unchanged in the binding region, but there is a large conformational change occurring in a more remote surface-loop region. It is suggested here that this loop could be important in complexation of AXT and contributes to the spectral properties. Also presented here is the first observation of single-crystal diffraction of the full 'α-crustacyanin' complex comprising 16 protein subunits and 16 bound AXT molecules (*i.e* eight β-crustacyanins) at 5 Å resolution. Optimization of crystallization conditions is still necessary as these patterns show multiple crystallite character, however, 10 Å resolution single-crystal diffraction has now been achieved. Provision of the new SRS MPW 10 and SRS MPW 14 beamline robotic systems will greatly assist in the surveying of the many α-crustacyanin crystallization trials that are being made. New solution X-ray scattering (SXS) measurements of β- and α-crustacyanin are also presented. The β-crustacyanin SXS data serve to show how the holo complex fits the SXS curve, whereas the apocrustacyanin A1 homodimer from the crystal data naturally does not. Reconstructions of α-crustacyanin were accomplished from its scattering-profile shape. The most plausible ultrastructure, based on a fourfold symmetry constraint, was found to be a stool with four legs. The latter is compared with published electron micrographs. A detailed crystal structure of α-crustacyanin is now sought in order to relate the full 150 nm bathochromic shift of AXT to that complete molecular structure, compared with the 100 nm achieved by the β-crustacyanin protein dimer alone. Rare lobster colourations have been brought to attention as a result of this work and are discussed in an appendix.

© 2003 International Union of Crystallography
Printed in Denmark – all rights reserved

1. Introduction

The role of *Acta Crystallographica Section D* has been to serve both as a focus for the reporting of methods developments and of new structures. In this article, as our contribution celebrating the tenth anniversary of *Acta Cryst. D*, we offer a case where a comprehensive battery of techniques is being applied to understand the colouration mechanism of the lobster carapace.

1.1. Biochemical background

1.1.1. Composition. As a primary colour, blue has been the most difficult for artists and scientists to create and Nature's blues are relatively rare (Ball, 2001).

Interest in the blue coloration of the shell of natural (*i.e.* uncooked) lobster *Homarus gammarus* (Fig. 1) was initiated by Newbigin (1897, 1898), who found that one of the group of pigments, now known as carotenoproteins, could be extracted with ammonium chloride and suggested that it was the result of a combination of a complex organic base and a lipochrome. Later, Verne (1921) correctly proposed that the pigment was a combination of a carotene-like compound and a protein. The carotenoid involved, astaxanthin (3,3′-dihydroxy-β,β-carotene-4,4′-dione; AXT; Fig. 2) which has a molecular weight of around 550 Da, was subsequently identified as the prosthetic group (Kuhn & Sorensen, 1938). Wald *et al.* (1948) extracted the predominant carotenoid complex from among other carotenoproteins in the carapace, established its proteinaceous nature and named it crustacyanin. Now we know that the native carotenoprotein, α-crustacyanin, has a molecular weight of about 320 kDa and that it is a multi-macromolecular 16-mer complex of protein subunits with 16 bound AXT molecules. These subunits are electrophoretically distinct components, each of approximate molecular weight of 20 kDa, classified by amino-acid composition, size estimation and peptide mapping into two groups: gene type CRTC, with protein modifications A1, C1 (predominant) and C2, and gene type CRTA, with protein modifications A2 (predominant) and A3 (Cheesman *et al.*, 1966, 1967; Kuhn & Kühn, 1967; Buchwald & Jencks, 1968). Combinations of pairs of these proteins, one from each group, are called β-crustacyanins; they occur naturally in lobster shell and are formed irreversibly by dissociation of α-crustacyanin. α-Crustacyanin is thus an octamer of heterodimeric β-crustacyanins (Fig. 3). The removal of the carotenoid prosthetic groups from either the β- or α-crustacyanins results in a reversible dissociation into the apoprotein subunits. Crystal structures of apocrustacyanin A1 (Cianci *et al.*, 2001), of apocrustacyanin C1 (Gordon *et al.*, 2001) and β-crustacyanin (A1; A3) (Cianci *et al.*, 2002) have so far been determined. The apoproteins crystallize as homodimers, whereas in solution they remain as monomers.

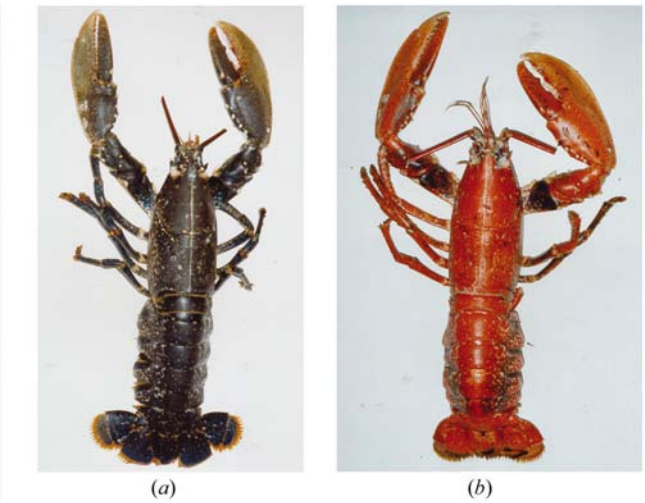

Figure 1
Photographs of the European lobster *H. gammarus*: (*a*) live, (*b*) after cooking. (We are grateful to Dr George Britton, University of Liverpool for these pictures.)

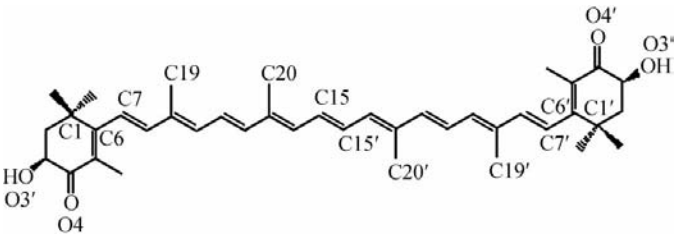

Figure 2
The chemical scheme of astaxanthin (3,3′-dihydroxy-β,β-carotene-4,4′-dione)

1.1.2. Spectral characteristics. The absorption spectrum of the carotenoid astaxanthin (Fig. 4) is bathochromically shifted by some 150 nm in α-crustacyanin (Wald *et al.*, 1948). The visible absorption spectrum of free AXT has λ_{max} = 472 nm (in hexane) or 492 nm (in pyridine), while the visible absorption spectra of bound AXT has λ_{max} 580–590 nm in the β-crustacyanins (*i.e.* a shift of 100 nm) or λ_{max} = 632 nm in α-crustacyanin (Buchwald & Jencks, 1968). The bathochromic shift in α-crustacyanin is dramatically evident when the lobster

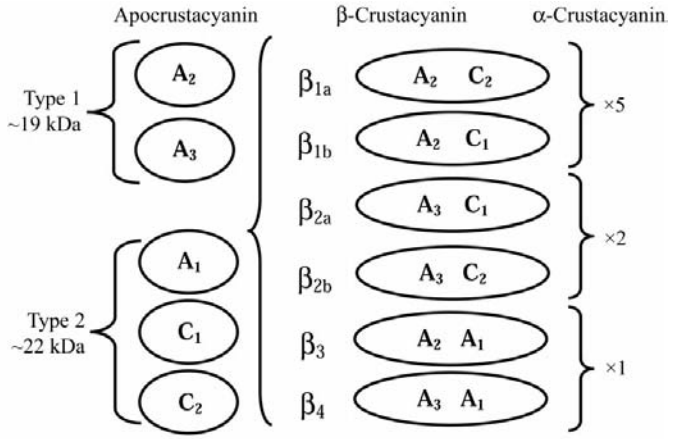

Figure 3
Illustration of the composition of α-crustacyanin. α-Crustacyanin is made of eight heterodimeric units called β-crustacyanin. Within one α-crustacyanin five units are type β1a and β1b, two units are type β2a and β2b, and one unit is either β3 or β4. β1a, β1b, β2a, β2b, β3 and β4 are different heteromeric combinations of apocrustacyanin type A1, A2, A3, C1 and C2 plus two bound astaxanthin molecules. This figure is courtesy of Boggon (1998).

changes its colour from slate-blue to orange–red on cooking. Interestingly, extracted α-crustacyanin goes red upon dehydration and on rehydration returns to blue (Cheesman *et al.*, 1966). The structural basis of the bathochromic shift mechanism has long been elusive. Moreover, the similarities in α-crustacyanin's absorption characteristics to the visual pigment rhodopsin provide an additional interest in these studies; the crustacyanin–astaxanthin complex could just be a very primitive photoreceptor system (North, 1993).

1.1.3. Dissociation and reconstruction. In general, crustacyanins are relatively stable complexes in the pH range 5–8.5. Dilute solutions of α-crustacyanin (0.1 mg ml^{-1}) lose only about 3% of absorbance at their respective λ_{max} on exposure to bright sunlight for 1 d. Formation of β-crustacyanin occurs spontaneously at a slow rate during storage of α-crustacyanin in buffer or under ammonium sulfate and in electrophoresis using a low ionic strength. α-Crustacyanin may be reconstructed from freshly prepared apoprotein and AXT. The ability to reconstruct the α-form is gradually lost on storage of the apoprotein in solution in a refrigerator or as a precipitate under 80% ammonium sulfate solution. Old preparations and freeze-dried apoprotein or recombination of astaxanthin with a mixture of individual apoprotein units give only β-crustacyanin and a product of apoprotein size with λ_{max} = 565 nm. When a solution of crustacyanin is dialyzed against several changes of distilled water, its colour changes to a distinct purple. Addition of inorganic salts restores the spectrum almost completely to the native α-crustacyanin form. Considerable salt concentration is necessary for complete restitution of the spectrum; with sodium chloride, this lies in the region of 0.075 *M*. Experiments with KCl, K_2SO_4 and $MgSO_4$ indicate that the cation is probably the determining factor of such restitution of the spectrum. While 0.02 *M* KCl and 0.01 *M* K_2SO_4 each gave about 65% restitution after 1 h, 0.01 *M* $MgSO_4$ gave almost complete recovery in the same period. It appears that α-crustacyanin cannot exist in its blue form at low ionic strength but is dissociated to the purple dimeric β-crystacyanin (Cheesman *et al.*, 1966; Zagalsky, 1985).

1.2. The carotenoid astaxanthin

1.2.1. Chemical properties. Carotenoids are a class of hydrocarbons (carotenes) consisting of eight isoprenoid units. These are joined in such a manner that the arrangement of isoprenoid units is reversed at the centre of the molecule. Carotenoids are natural fat-soluble pigments found ubiquitously in nature in plants and algae and in ornamental and tropical fish, where they are responsible for various species-related yellow, red and related colours. In photosynthetic bacteria, they play a critical role in the photosynthetic process. Carotenoids are also found in some non-photosynthetic bacteria, such as yeast and moulds, where they may be responsible for protection against light or oxygen. Within animals, carotenoids serve as antioxidants or as pro-vitamin A (Britton *et al.*, 1994) and in marine invertebrates, particularly crustacea, provide their spectacular colourations (blues, purple, orange, red) often by combination with protein. Carotenoids also play an important potential role in human health by acting as biological antioxidants, thus protecting cells and tissues from the damaging effects of free radicals and singlet oxygen. An example is lycopene, the carotenoid responsible for the red colour of tomatoes, which is particularly effective at quenching the destructive potential of singlet oxygen (Di Mascio *et al.*, 1989). Free radicals and singlet oxygen have been linked to a number of pathological conditions including aging (Harman, 1981), artherogenesis (Steinberg *et al.*, 1989) and carcinogenesis (Moody & Hassan, 1982; Marnett, 1987). Because of their various biological and nutritional roles, a variety of carotenoids, both synthetic and naturally occurring products, are available on the market for the use in aquaculture and amongst them AXT is the predominant one (Meyers, 1994). AXT (Fig. 2) has been found to be essential for the proper growth and survival of a variety of crustaceans such as shrimp, crawfish, crab and lobster (Torrissen & Christiansen, 1995). AXT is itself a powerful antioxidant. It is active as a potent quencher of singlet oxygen and has a strong scavenging effect against free radicals (Miki, 1991).

1.2.2. Conformation and structure. The analyses of the crystal structures of β-carotene (Sterling, 1964) and of canthaxanthin (Bart & MacGillavry, 1968) provided the conformation of these molecules. The canthaxanthin crystals were highly dichroic in polarized light, varying between light red and dark red (Bart & MacGillavry, 1968). The studies showed that the single and double bonds clearly alternate in double- and single-bond character. There is no sign of a mixed bond nature. The polyene chain has the all-*trans* configuration. The canthaxanthin chain is doubly curved (see Fig. 3 in Bart & MacGillavry, 1968).

Since large differences in packing are found between these crystal structures, but they consistently show a similar conformation, it seems that the in-plane bending of the fully conjugated polyisoprenoid chain arises from intramolecular forces. Hence, the similar conformation of AXT inferred from these crystal studies can also be expected to exist in solution.

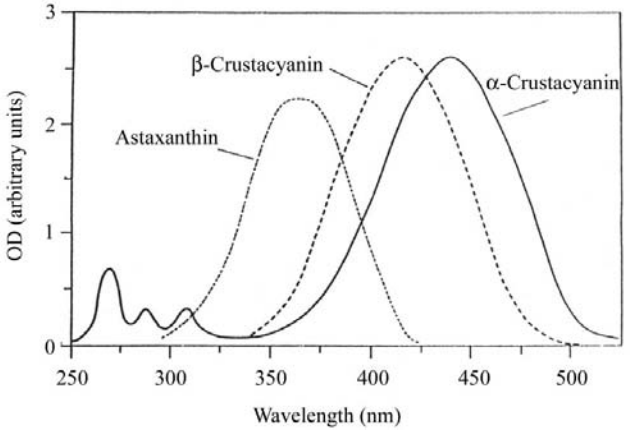

Figure 4
Absorption spectra: astaxanthin in hexane, β-crustacyanin, α-crustacyanin.

The major differences between the free and the crystallized molecule will be found where the packing forces affect the structure. For example, both crystal structures show the carotenoids having the s-*cis* arrangement about the C6—C7 bond with an angle of −43° (β-carotene) and −56° (canthaxanthin) between the best planes through C7═C8 and C5═C6 (double-bond system) and C6═C5—C4═O (cyclohexenone ring). The similarity in the packing of β-carotene and canthaxanthin is that the chain centres are packed in a grid so that there is contact between approximately coplanar chains through interlocking of the side-chain methyl groups C19 and C20. There is also a backbone contact between one chain and the one above and/or below, with average distances of 3.5 Å between them.

1.3. A proposed three-dimensional structure of β-crustacyanin

A putative tertiary structure of β-crustacyanin was proposed (Keen *et al.*, 1991*a*,*b*) as a molecular model based on the coordinates from the solved crystal structures of retinol-binding protein (Newcomer *et al.*, 1984), β-lactoglobulin (Papiz *et al.*, 1986) and bilin-binding proteins (Huber, Schneider, Epp, Mayr, Messerschmidt *et al.*, 1987; Huber, Schneider, Epp, Mayr, Muller *et al.*, 1987; Holden *et al.*, 1987). The predicted structures of both subunits, A2 and C1, have a β-barrel structure typical of the lipocalins and consisting of eight antiparallel β-strands arranged in two orthogonal β-sheets to form a calyx. A model for the dimer β-crustacyanin was also suggested formed by the two subunits with their associated AXTs. The model was based on the dimer of the bilin-binding protein of *Pieris brassicae*, the crystal structure of which had been solved by Huber and coworkers (Huber, Schneider, Epp, Mayr, Messerschmidt *et al.* 1987; Huber, Schneider, Epp, Mayr, Muller *et al.*, 1987). The suggested heterodimer, produced by the head-to-head association of C1 and A2 monomers, indicated that the carotenoids were shielded from the aqueous environment. The proposed locations of the carotenoids placed them at an angle of 58° with respect to one another and at a centre-to-centre distance of about 15 Å. The astaxanthin β-ionone ring was positioned within each calyx of C1 and A2, as deep into the cavity as contacts would permit. The β-ionone ring would thus lie close to the conserved Trp35 (C1) or Trp30 (A2) at the bottom of the calyx of each proposed protein model, using the 4-oxo group to interact with the surrounding residues *via* a network of hydrogen bonds. The angles between the β-ionone rings and polyene chains were set at −55°, close to those observed in the crystal structure of the 4,4′-dioxo-carotenoid canthaxanthin (−52° and −56°; Bart & MacGillavry, 1968).

1.4. Chemical studies on the mechanism of the bathochromic shift

As noted in §1, the bathochromic shift of the astaxanthin absorption of lobster crustacyanin has intrigued scientists for over 50 years (Wald *et al.*, 1948; Buchwald & Jencks, 1968; Salares *et al.*, 1979; Britton *et al.*, 1995). Prior to the X-ray crystallographic investigation of β-crustacyanin (Cianci *et al.*, 2002), detailed chemical studies had been the main way to investigate the chemical mechanism, which are now summarized.

1.4.1. Chemical reconstitution with modified carotenoids in the study of the bathochromic shift. Chemical reconstitution studies with a range of natural and chemically synthesized carotenoids have established the essential chemical characteristics of a carotenoid to produce this bathochromic shift effect (Britton *et al.*, 1995). Only normal C40 carotenoids in the all-*E* (all-*trans*) configuration are bound to the apo protein and no great variation in overall shape and size of the carotenoid is tolerated. Both 4 and 4′ keto groups are essential for the formation of purple β-crustacyanin-type complexes: they are likely to be conjugated with the polyene chain. Hydroxy groups at these positions are not effective. The efficiency with which the 4,4′-diketocarotenoids are bound to the protein is greater when hydroxy groups are present at C3 and C3′. The chirality of these hydroxy groups is not important; (3*R*-3′*R*)-, (3*R*-3′*S*)- and (3*S*-3′*S*)-astaxanthin all give similar β-crustacyanin products in similar yields. The hydroxy groups are not involved in the spectral shift mechanism, but the increased polarity may make it easier for the end groups to be positioned correctly in the binding site. The central C20, C20′, C19 and C19′ methyl groups must also be present and it has been suggested (Britton *et al.*, 1995) that these are involved in essential steric interactions that maintain the chromophore in the correct position and conformation (Britton *et al.*, 1995).

1.4.2. Circular-dichroism studies. For free carotenoids, including AXT, circular dichroism (CD) in the visible region generally has very weak absorption bands, but in the UV region it is characterized by a series of bands of alternating sign, *i.e.* positive below λ_{max}, negative above λ_{max} and 0 near, not exactly at, λ_{max}. In the CD spectrum of natural α-crustacyanin there are again several bands of alternating sign in the UV region, but the main feature is now a strong CD in the visible region absorption band. The CD spectrum of the β-crustacyanin dimer is similar to that of α-crustacyanin, allowing for the difference in λ_{max}, but is of lower amplitude. In both cases the main CD band shows a change of sign at λ_{max} and evident exciton splitting, indicating that the two AXT molecules in each β-crustacyanin dimer are proximal enough to interact energetically (Buchwald & Jencks, 1968; Britton *et al.*, 1995).

1.4.3. Resonance Raman studies. Resonance Raman spectra of crustacyanins generally support an electron-redistribution mechanism (*i.e.* polarizing one half of the astaxanthin from the other) for the bathochromic shift and argue against a large protein-induced distortion of the polyene chain, although minor changes to its geometry have been suggested (Salares *et al.*, 1979; Britton *et al.*, 1995). These results are in contrast to the β-crustacyanin crystal structure (Cianci *et al.*, 2002).

1.4.4. ^{13}C MAS NMR with Stark spectroscopy studies. ^{13}C MAS NMR together with Stark spectroscopy results suggest an essentially symmetrical polarization of the AXT in

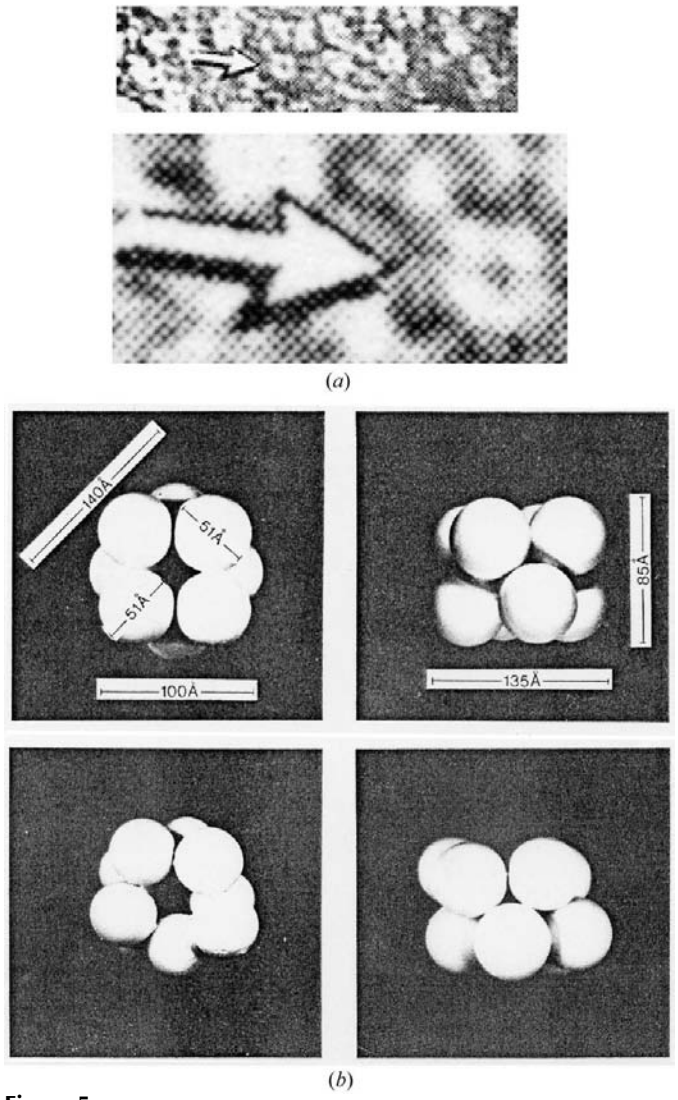

Figure 5
Electron micrographs of α-crustacyanin (*a*). (*b*) Proposed schematic model for the quaternary structure of α-crustacyanin. Each sphere represents a β-crustacyanin. Top, double tetramer; bottom, helical coil. Reprinted from Zagalsky & Jones (1982), copyright (1982) with permission from Elsevier.

crustacyanin with some asymmetry superimposed on the two halves of the chromophore (Krawczyk & Britton, 2001; Weesie *et al.*, 1997). The study of [14,14′-^{13}C2]-AXT showed significant differences between the spectra of the free and complexed AXT. In fact, the signal for C14 and C14′ of the complex was split into two components with a significant downfield shift compared with that of free AXT, from 134.1 p.p.m. to 138.0 and 140.9 p.p.m.

The line widths of the two components were different. This means that C14 and C14′ of AXT are in dissimilar protein environments; the electron charge densities at C14 and C14′ are not identical and both are different from those in free AXT (Weesie *et al.*, 1995). Similar results were obtained with [12,12′-^{13}C2]-AXT. In contrast, the signals for [13,13′-^{13}C2]-, [15,15′-^{13}C2]- and [20,20′-^{13}C2]-AXT all showed a small upfield shift owing to protein binding (Weesie, Merlin, De Groot *et al.*, 1999). The differences in electronic charge density are consistent with polarization from both ends of the molecule. The effect is quantitatively different in the two halves of the AXTs, showing that the carotenoids are in an asymmetrical arrangement. The bathochromic shift was attributed, on this basis, to perturbation of the ground-state electronic structure of the carotenoid caused, for example, by protonation of the C4 and C4′ C=O groups (Weesie *et al.*, 1997) and this polarization was supported by quantum-mechanical calculations (Weesie, Merlin, De Groot *et al.*, 1999; Weesie, Merlin, Lugtenburg *et al.*, 1999). Prior to determination of the crystal structure, the proposed model for the β-crustacyanin (Keen *et al.*, 1991*b*) had an end ring in a non-polar non-proton environment. This would be inconsistent with the polarization introduced by protonation of the C4 and C4′ keto groups *via* a charged amino-acid residue. It was also suggested that a water molecule is involved somehow in the polarization process owing to the dehydration/rehydration colour-change effect (Britton *et al.*, 1995). Just how the carotenoid is bound in the complex only became apparent from the crystal structure of β-crustacyanin and is discussed in §3.

1.4.5. Quaternary structure. An early electron-micrograph study of α-crustacyanin (Zagalsky & Jones, 1982; Fig. 5) revealed several different structures consistent in size with the value of the Stokes radius of the protein, 73 Å. These included diffuse rings and both four- and five-sided structures, composed of four, six or an indefinite number of subunits of β-crustacyanin size. One possible subjective interpretation is of a compact double tetrameric structure in which the two tetramers are face to face, with the subunits of one positioned in the grooves between the subunits of the other. An alternative is a linear array of eight β-crustacyanin molecules coiled in a helical manner into a compact configuration, of between four and five subunits per turn, in which the subunits of the second turn of the helix lie in the grooves of those of the first. If viewed at different angles, such structures would provide the observed electron-micrograph patterns. No doubt other equally feasible models can be conceived. The helical arrangement is supported in small-angle X-ray scattering of α- and β-crustacyanin (Dellisanti *et al.*, 2003). An alternative possible structure is discussed below.

2. The crystallography challenge of crustacyanin

Whilst crystals of the apocrustacyanin C2, C1 and A1 as well as β-crustacyanin had been known for some time (Wright *et al.*, 1992; Chayen, Gordon & Zagalsky, 1996; Chayen *et al.*, 2000; Chayen, Gordon, Phillips *et al.*, 1996) these structures had not been solved. The problematic nature of the structure solution of these proteins warranted consideration and development of new approaches. Three putative disulfides per protein subunit were likely to exist, based on molecular homology modelling against known lipocalin protein structures.[1] With two such subunits per crystallographic asymmetric unit this direct approach was still difficult; it involved detecting

[1] The A3 sequence published after the determination of the β-crustacyanin has an incorrect assignment of residue 147 as Ser. Further investigation into the disulfide bridges revealed this residue to be a Cys.

a weak signal from these sulfurs and suggested the use of softer X-rays, combined with high data redundancy, as we reported (Chayen *et al.*, 2000) based on work at SRS. We have recently described the structure solution of CRTC in the form of the A1 dimer using softer X-rays (2 Å wavelength; Cianci *et al.*, 2001). This provided the breakthrough needed for the β-crustacyanin complex structure determination (Cianci *et al.*, 2002). The A1 structure solution required a native data set and a data set with an optimized xenon $L_{\rm I}$ edge f'' signal recorded at 2 Å wavelength. The hand of the xenon SIROAS A1 crystal structure phases was determined by using the sulfur anomalous signal from a very high redundancy native data set also recorded at 2 Å wavelength. For refinement, a high-resolution data set, at 1.4 Å resolution, was measured at short wavelength. These data sets were collected at 100 K with a crystal frozen in a loop. This A1 structure was then used as a search motif in the structural studies of the dimeric form, β-crustacyanin, which contains two bound AXT molecules (Cianci *et al.*, 2002); see §3.

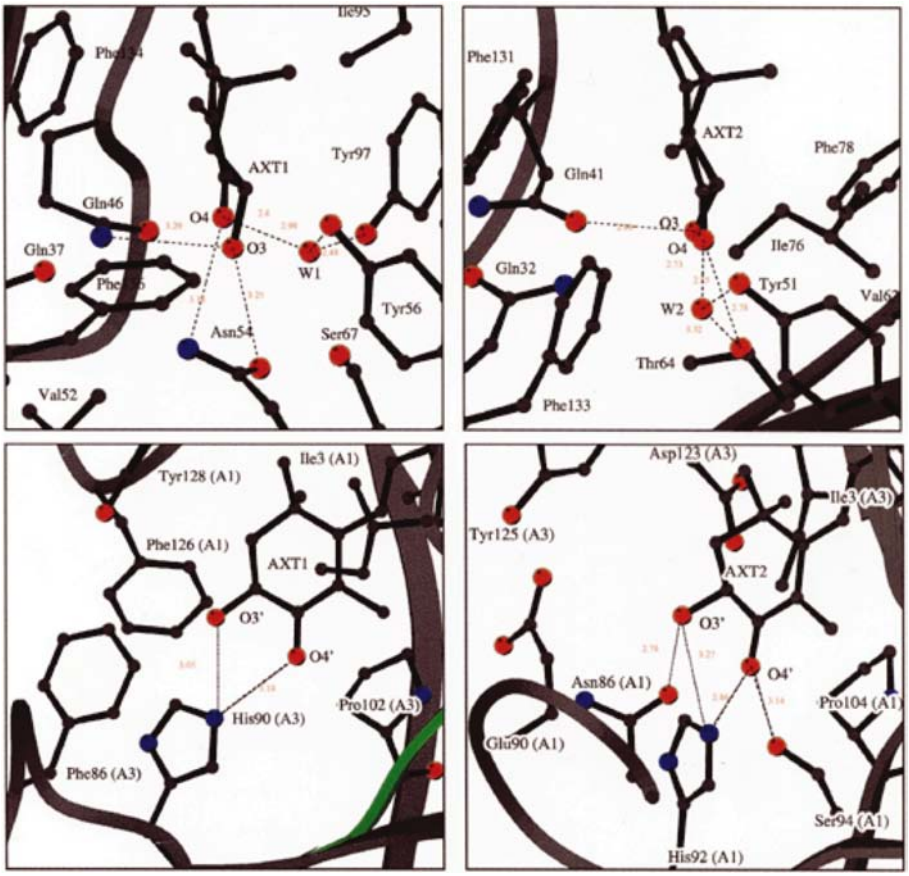

Figure 6
The detailed layout of the astaxanthin-binding sites at the end-ring molecular environments in β-crustacyanin (based on the crystal structure presented in Cianci *et al.*, 2002). Top left: C1–6 end ring of AXT1 bound to A1 molecule; top right: C1–6 end ring of AXT2 bound to A3 molecule; bottom left: C1′–6′ end ring of AXT1 bound to A3 molecule; bottom right: C1′–6′ end ring of AXT2 bound to A1 molecule. Each astaxanthin molecule is equally shared between the two subunits A1 and A3. (Copyright, 2002, National Academy of Sciences USA.)

3. The structural details of the AXT binding in β-crustacyanin

In the crystal structure of β-crustacyanin, one end of each AXT (Fig. 6) lies within the calyx of its respective lipocalin partner with the C4-keto group linked to a protein bound water molecule by a short hydrogen bond within the hydrophobic cavity. The opposite end of each AXT is connected to the neighbouring lipocalin subunit, thereby cementing the dimer, with the C4′ keto group close to the NE2 of a His residue in each case. Although the latter sites are mainly hydrophobic, one is more accessible to water than the other. The C20- and C20′ methyl groups, essential features of the carotenoid structure for protein binding, are firmly embedded in a jigsaw-like manner in the protein structure. In the combination, all four β-ionone rings are essentially coplanar with the main polyene chain, with marked and similar bowing of each AXT; the AXT approach within 7 Å at their centres, as predicted from the CD spectrum (Gardiner & Thomson, unpublished work; cited in Zagalsky, 1976). In the unbound state the β-ionone rings of AXT are out of the plane of the polyene chain, with dihedral angles of $\sim -43^\circ$ owing to steric hindrance between the C5 methyl and C8 hydrogen. The ring keto groups and C5═C6 and C5′═C6′ are consequently only partially conjugated with the polyene chain. One of us has presented an analysis of the component bathochromic shift effects based on a variety of carotenoid types (Zagalsky, 2003). Quantum calculations predicting the UV–visible spectral shift by Durbeej & Eriksson (2003) present a preference for the bathochromic shift effect arising from a protonated histidine present at one end of each AXT, rather than the increased conjugation arising from co-planarization of the end rings of each bound AXT.

3.1. Structural comparisons of the A1 monomer in β-crustacyanin *versus* A1 in the unbound form

The availability of models of the apocrustacyanin A1 homodimer and the β-crustacyanin (A1/A3 heterodimer) (Cianci *et al.*, 2001, 2002) allow comparisons to be made of the A1 monomer in its bound and unbound forms. A similar comparison for A3 in its bound and unbound forms is not yet possible since the structure of the carotenoid-free form is not known. The r.m.s. values for the C^{α}-atom trace of the β-crustacyanin monomer A1 *versus* the A1 monomers *A* and *B* in the homodimer are 1.66 and 1.65 Å, respectively. In both, the main differences are concentrated in the N-terminal helix comprised of residues 2–14 and residue Ile122 (β-strand *G*). It appears that upon binding of the astaxanthin molecules and

hetero-dimerization of A1 with A3, the N-terminus moves from its position to cover an exposed side of the carotenoid without any consequent change of its secondary structure. This behaviour (ligand-induced conformational change) has been observed in other lipocalins, *e.g.* RBP (Zanotti *et al.*, 1993). The movement of Ile122 is also of interest because it appears to occur owing to the presence of the two carotenoids, bringing Ile122 right into the middle of the two AXTs. In this position Ile122 works as a wedge between the two carotenoids.

The r.m.s. values calculated for the position of the side-chain atoms of β-crustacyanin monomer A1 *versus* A1 monomers *A* and *B* in the homodimer are 2.64 and 2.60 Å, respectively. Among all the residues displaying the largest r.m.s. values are Asp16 (loop), Asn29 (loop), Lys61 (loop), Lys66 (β-strand *C*), Arg79 (β-strand *D*), Glu98 (loop), Phe101 (loop), Phe126 (loop), Asp144 (loop) and Lys148 (α-helix). Of these, the ones not exposed on the surface of the protein are Arg79, Glu98, Phe101 and Phe126. Of the four residues, only Phe101 is conserved in CRTA.

The A1 bound form in the β-complex shows the side chain of Arg79 to be close to AXT1 C3 and it proved to have a certain degree of freedom in both monomers of the A1 unbound form, where it displays a double conformation. Glu98 is close to the cavity where AXT1 is bound. Phe101 rearranges the position of its aromatic ring upon binding of the carotenoid. Phe126 participates in the formation of the binding site of AXT1 at the interface between A1 and A3 monomers. Arg79, Glu98 and Phe101 already proved to have a certain degree of movement from the comparison between A1 and C1 dimers (Cianci *et al.*, 2001; Gordon *et al.*, 2001). This is clearly demonstrated *via* the movie made by linear interpolation between the unbound and bound A1 protein structures (see supplementary material[2]).

4. First ever diffracting crystals of α-crustacyanin

The initial conditions for crystallization of α-crustacyanin were found using commercial products such as the Hampton Crystal Screens. The protein readily produces needle/rod-shaped crystals with tapered ends, which give no diffraction at all even with intense synchrotron radiation at SRS MPW14.2 (Fig. 7*a*). Efforts to optimize the conditions involved hundreds of trials testing a range of temperatures (between 277 and 293 Å), a wide range of additives and varying the concentrations of the protein and crystallizing agent. Trials were performed using both microbatch and vapour-diffusion (hanging drops) methods. The presence of zinc produced small crystals, which looked like rectangular blocks, but these shattered when removed from the droplet. Even larger crystals, which were more robust and could withstand harvesting, produced no diffraction. Trials which involved the separation of the stages of nucleation and growth by starting the crystallization process at conditions that promote nucleation and then backing off at given times after setup, provided information on the conditions which were metastable. Conditions just above the metastable ones produced single-looking plates (Fig. 7*b*), which took longer to grow but showed some diffraction to 12 Å resolution even 5 Å. This was the first time that any diffraction was observed for α-crustacyanin crystals (Figs. 8*a* and 8*b*)!

Further optimization was necessary. Glycerol has been used routinely with other proteins for cryoprotection in order to avoid ice rings in the diffraction pattern. It also acts to slow down the crystallization and therefore improve crystal quality. It was added to the α-crustacyanin crystallization trials at different concentrations (5–20%). Initially, it produced a larger number of smaller crystals compared with the controls, but these crystals increased in size more slowly than those in the trials containing no glycerol. Crystals containing 20% glycerol diffracted to 10 Å, but importantly as single-

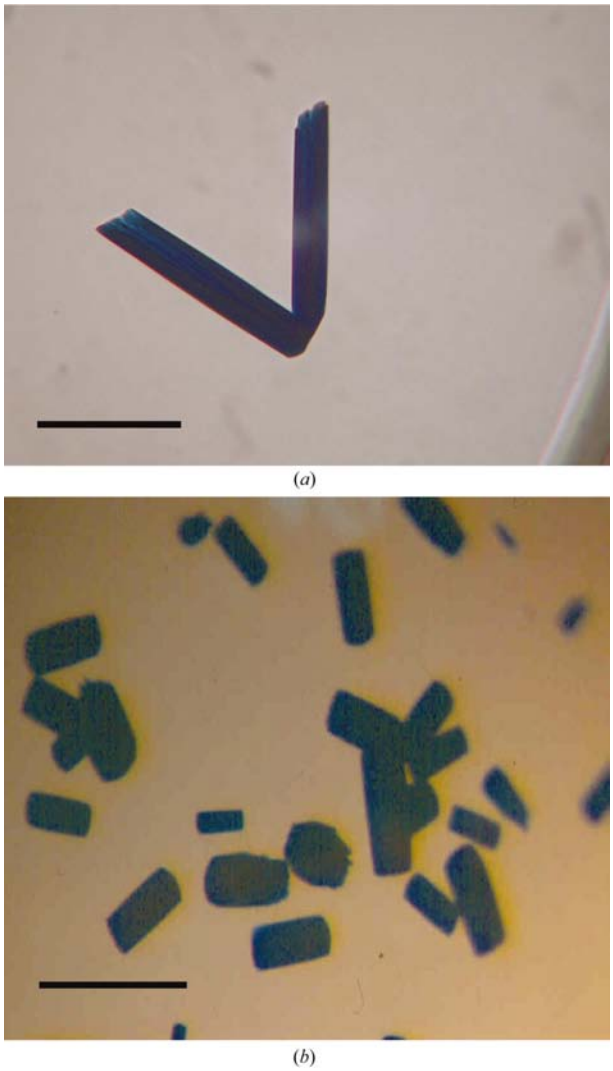

Figure 7
α-Crustacyanin crystals. (*a*) Initial experiments. These crystals produced no diffraction. (*b*) Crystallization conditions deliberately involving glycerol to slow crystal growth. Crystals typical of those that gave diffraction to about 10 Å are shown. The crystallization trials contained 20% glycerol. Scale bars are 100 µm.

[2] Supplementary material has been deposited in the IUCr electronic archive (Reference: GR5000). Details for accessing this material are described at the back of the journal.

crystal diffraction rather than multiple-crystallite diffraction (Fig. 8*c*).

5. Solution X-ray scattering of α-crustacyanin

Besides electron microscopy and, in the longer term, crystallography, another way to discern the structural layout of the full complex is *via* solution X-ray scattering (SXS). The molecular weight of the complex, at 320 kDa, and its undefined composition challenge the methods. We have initiated SXS experiments, including both the small and the wider angle region, and applied symmetry constraints from the electron micrographs. This analysis is ongoing and a brief overview is given here. In addition, Dellisanti *et al.* (2003) have also investigated the complex with SXS and have recently published their analysis, which also used the electron-micrograph constraints. In their case they instead assume a possible helical layout proposed as an option by Zagalsky & Jones (1982). Dellisanti *et al.* (2003) have thus presented evidence of the α-crustacyanin being of cylindrical shape with axial length 238 Å and a radius of 47.5 Å, in a helical arrangement, pointing out that 'the complexity of this non-globular scaffolding containing many discontinuities as well as the relatively large size of the protein (2840 residues) may be the reasons why the classical *ab initio* shape restoration programmes have, unfortunately, in this case been exceeded'. In our case we also harnessed the electron-micrograph information of Zagalsky & Jones (1982), but with the option of a fourfold look to the electron micrographs and thereby applied that symmetry constraint instead. Grossmann and coworkers' SXS measurements on SRS station 2.1 (Fig. 9; Grossmann *et al.*, work to be published) conclude that evaluation with a plausible 'piano-stool' layout (see inset views in Fig. 9) interpretation. This has approximate dimensions 80 Å across the top of the stool, 150 Å high and 130 Å wide, between the splayed legs of the stool. The overall diagonal maximum dimension would be 220 Å. This is at variance with the option that Dellisanti *et al.* (2003) have favoured. Even though our

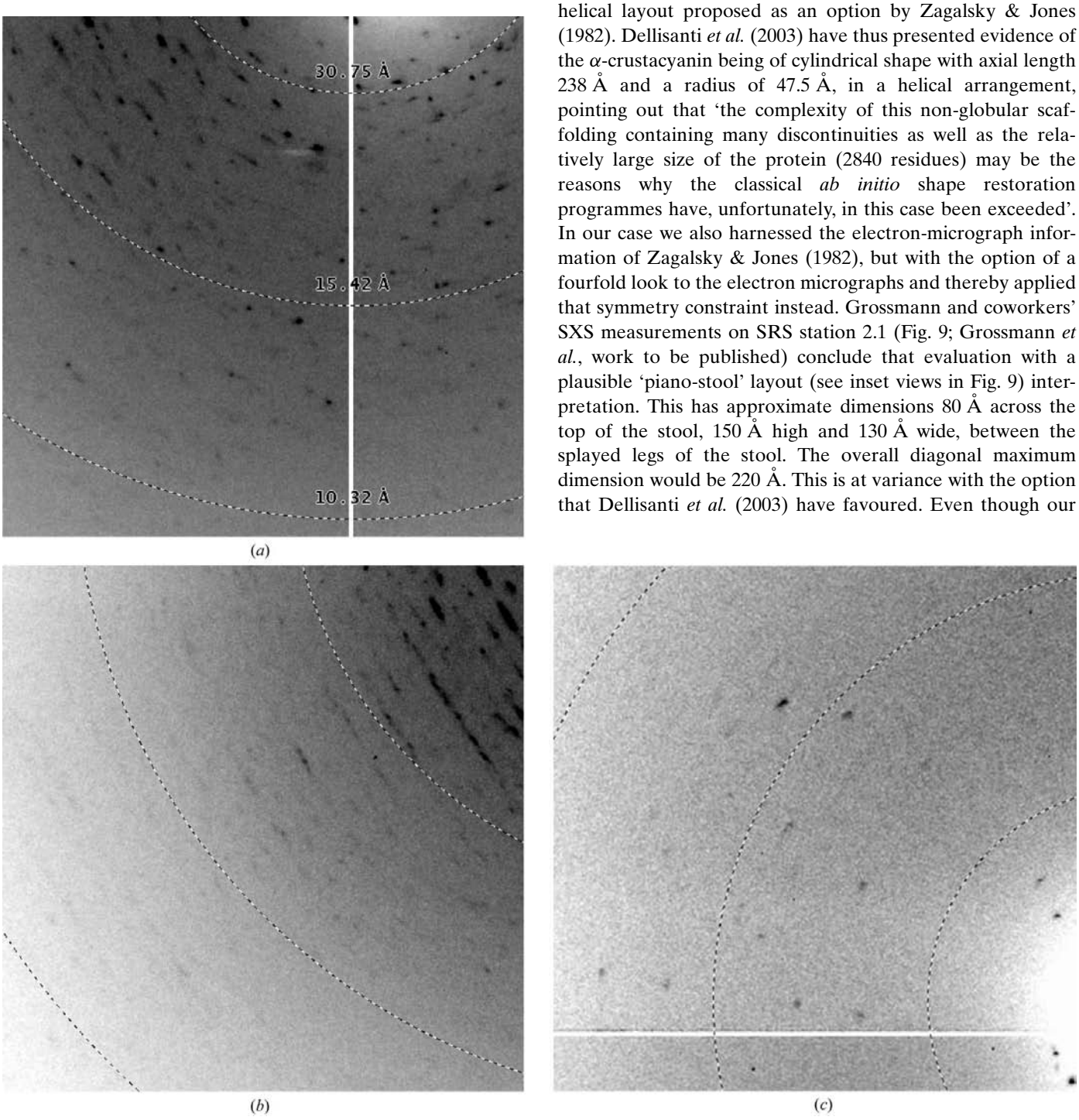

Figure 8
α-Crustacyanin diffraction patterns. (*a*) From crystals of Fig. 7(*a*) type and zoom into centre of pattern (*b*) and one corner (resolution rings being 15.42, 10.32 and 5 Å). (*c*) Single-crystal patterns can be obtained from some crystals but only to 10 Å.

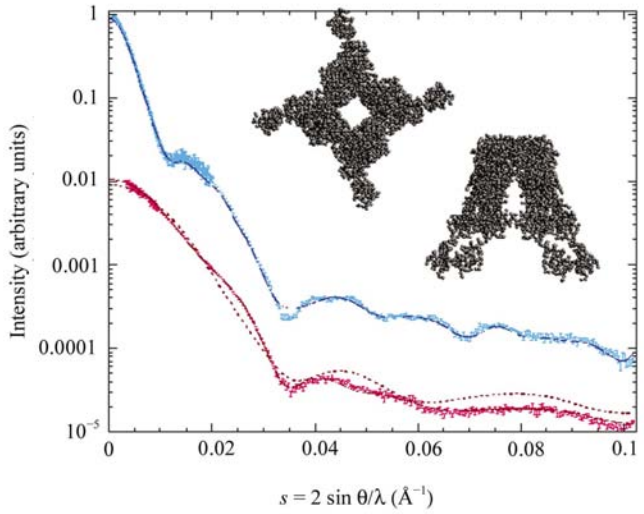

Figure 9
X-ray scattering data measured at the Daresbury SRS station 2.1 from solutions of α-crustacyanin (blue error bars) and β-crustacyanin (red error bars) as a function of the momentum transfer s (which is defined by the X-ray wavelength λ and the scattering angle 2θ). The curves have been displaced for better visualization. The smooth curve fitting the α-crustacyanin scattering profile results from a shape restoration with fourfold molecular symmetry. The inset depicts a representative shape model in two orthogonal orientations highlighting the 'piano-stool' layout. Each amino acid of full-length crustacyanin is represented by a sphere. In contrast, the red curve superimposed on the β-crustacyanin profile results from a scattering pattern simulation using the β-crustacyanin crystal structure of Cianci *et al.* (2002). The dotted curve representing the simulation based on the A1 homodimer of Cianci *et al.* (2001) clearly provides a very poor fit to the experimental data as expected.

shape restorations from the scattering data consistently produce comparable versions of the piano-stool arrangement, we too would conclude that improvements in cryo-EM offer the way to better define a low-resolution envelope to assist the SXS data interpretation. These efforts are an interim towards a full crystallographic analysis (see §4). However, in addition the proof that the full complex in solution has the same structure as in the solid-state crystal structure will be an important confirmation of the crystal structure relevance to the *in vivo* state in the lobster carapace. In addition, Fig. 9 shows the measured SXS curve for the β-crustacyanin (A1, A3) in solution and the excellent fit of the β-crustacyanin (A1, A3) crystal structure to that of Grossmann and coworkers. These structural details are sought so as to explain the final 50 nm bathochromic shift stemming from the complexation of the eight β-crustacyanins. Cianci (2002) has commented on different kinds of final plausible twistings of the astaxanthin conformations as a result of complexation of the β-crustacyanins into the α-crustacyanin.

6. Summary and conclusions

The following has been discovered from the β-crustacyanin and apocrustacyanin A1 crystal structures thus far.

Figure 10
Rare lobster colours. (*a*) Light blue *versus* the common blue/black. (*b*) Orange. Courtesy of the Maine Environmental Research Center, USA, to whom we are very grateful.

(i) The structural dimerization in the complex is different from the apocrustacyanin homodimer, *i.e* which must be a consequence therefore of the influence of the astaxanthins on the dimerization process (of the A1 with A3 subunits).

(ii) Comparison of the A1 unbound and A1 bound structures reveals extensive conformational change at one end of the binding site suggesting an 'induced fit' and at the other end of the 'molecular-recognition' binding site a 'lock-and-key' fit. This is interesting in general terms as the recognition of the astaxanthin molecule proceeds by both of these well known molecular-recognition phenomena.

(iii) There is a hydrophobic patch on the β-crustacyanin protein surface suggesting an oligomerization site for the α-crustacyanin.

(iv) In the colouration mechanism, we see that the clamping of the astaxanthin end rings are especially implicated (Cianci *et al.*, 2002; Clayden *et al.*, 2001). There is also, however, the pivotal placement of the two bound waters (one at each AXT keto oxygen, one end only) thus possibly linking to the dehydration colour-change effect. A favoured explanation of the basis of the colouration mechanism from past work is that the bound carotenoid is electronically polarized. Indeed, the β-crustacyanin crystal structure does also reveal a histidine at one end of each carotenoid. To define the protonation state of these two histidines structurally requires either an ultrahigh-resolution X-ray crystal structure and/or a neutron protein crystal structure. Unfortunately, the current diffraction resolution and small size of the β-crustacyanin crystals precludes either study. The fact that the crystals themselves are blue, even though they grow at pH 8 and that the protein colour is stable up to pH 8.5, makes it unlikely if not impossible that the histidines are positively charged; it depends on the pK_a of the buried histidines. Moreover, there are no obvious counterbalancing negatively charged residues nearby. Also problematic for the electronic polarization hypothesis is the 565 nm λ_{max} of the separate apoproteins with bound AXT (Quarmby *et al.*, 1977), in the monomeric form, *i.e.* thereby lacking the His binding from a subunit partner as in β-crustacyanin.

Targets for futher investigation include the following.

(i) The full α-crustacyanin complex crystal structure is sought in order to understand the final 50 nm of the bathochromic shift beyond that seen with β-crustacyanin. The details of the protein-subunit interactions are also sought and, in particular, the reason why β-crustacyanin is an irreversibly

formed dissociation product of α-crustacyanin, *i.e.* β-crustacyanin will not reform α-crustacyanin after dissociation.

(ii) Other marine animal colouration biological phenomena, including carotenoproteins from different invertebrate phyla having non-lipocalin partners, await investigation.

(iii) Biotechnology manipulation of the bathochromic shift in β-crustacyanin can now be investigated by protein-engineering methods.

APPENDIX *A*
The media interest in the β-crustacyanin crystal structure and variable lobster colourations

We found ourselves exciting much interest on the topic of colouration of astaxanthin in its bound and unbound forms. In layman terms the question 'Why does lobster change colour on cooking?' proved irresistible to the media. The TV news reported a new method of delivering the antioxidant, possibly cancer-preventing, astaxanthin molecule, which is hydrophobic unless bound to a protein (such as β-crustacyanin). Newspapers referred to the chance to use protein engineering and site-specific mutagenesis to alter the molecular-recognition site of astaxanthin and thus manipulate the colour; *i.e.* lessons in colour technology may find application in food colorants or designed new-coloured genetically modified flowering plants. High-school students formed a 'second wave' of interest with e-mailed requests to help them with the details of our research article so as to complete their chemistry homework assignments; Swiss-Prot (Gerritsen, 2002) provided an excellent resumé to e-mail out at that time. Later came more detailed science writer articles, such as Day (2002), including a description of the molecular basis of the narrowing of the energy gap between the highest occupied and the lowest unoccupied molecular orbitals. The technical breakthrough of using softer X-ray crystallography and xenon with sulfur anomalous scattering, reported in *Acta Crystallographica Section D*, along with the first new protein structure solved that way, was also highlighted.

A USA radio listener and also Charles Day of *Physics Today* drew our attention to the Marine Research Center in Maine, which has a collection of unusual coloured lobsters (Fig. 10). Are these rare lobster shell colorations the result of point mutations affecting the crustacyanin protein binding of the astaxanthins or point mutations preventing the oligomerization of the eight β-crustacyanins to form the α-crustacyanin? The elaboration of such a relationship would require purification of protein from a rare-colour lobster and then a protein crystal structure analysis of *e.g.* its β-crustacyanin.

We thank The Leverhulme Trust for support of the lobster crustacyanin research, SRS Daresbury Laboratory is thanked for the SR beamtime on MPW 14. SRS MPW MAD 10 is funded by BBSRC, EPSRC and MRC. MC was funded on an EPSRC Research Studentship for the work reported in Cianci *et al.* (2001, 2002).

References

Ball, P. (2001). *The Times*, T2, November 19, pp. 10–11.
Bart, J. C. J. & MacGillavry, C. H. (1968). *Acta Cryst.* B**24**, 1587–1606.
Boggon, T. J. (1998). PhD thesis. University of Manchester, England.
Britton, G., Liaaen-Jensen, S. & Pfander, H. (1994). Editors. *Carotenoids*, Vol. 1A, *Isolation and Analysis*. Basel: Birkhauser.
Britton, G., Weesie, R. J., Askin, D., Warburton, J. D., Gallardo-Guerrero, L., Jansen, F. J., de Groot, H. J. M. & Lugtenburg, J. (1995). *Carotenoids*, Vol. IB, *Spectroscopy*, edited by G. Britton, S. Liaaen-Jensen & H. Pfander, ch. 2, pp. 69–73. Basel: Birkhauser.
Buchwald, M. & Jencks, W. P. (1968). *Biochemistry*, **7**, 844–859.
Chayen, N. E., Cianci, M., Olczak, A., Raferty, J., Rizkallah, P. J., Zagalsky, P. F. & Helliwell, J. R. (2000). *Acta Cryst.* D**56**, 1064–1066.
Chayen, N. E., Gordon, E. J., Phillips, S. E. V., Saridakis, E. E. G. & Zagalsky, P. F. (1996). *Acta Cryst.* D**52**, 409–410.
Chayen, N. E., Gordon, E. J. & Zagalsky, P. F. (1996). *Acta Cryst.* D**52**, 156–159.
Cheesman, D. F., Lee, W. L. & Zagalsky, P. F. (1967). *Biol. Rev.* **42**, 132–160.
Cheesman, D. F., Zagalsky, P. F. & Ceccaldi, H. J. (1966). *Proc. R. Soc. London Ser. B*, **164**, 130–151.
Cianci, M. (2002). PhD thesis. University of Manchester, England.
Cianci, M., Rizkallah, P. J., Olczak, A., Raftery, J., Chayen, N. E., Zagalsky, P. F. & Helliwell, J. R. (2001). *Acta Cryst.* D**57**, 1219–1229.
Cianci, M., Rizkallah, P. J., Olczak, A., Raftery, J., Chayen, N. E., Zagalsky, P. F. & Helliwell, J. R. (2002). *Proc. Natl Acad. Sci. USA*, **99**, 9795–9800.
Clayden, J., Greeves, N., Warren, S. & Wothers, P. (2001). *Organic Chemistry*. Oxford University Press.
Day, C. (2002). *Phys. Today*, **55**, 22–23.
Dellisanti, C. D., Spinelli, S., Cambillau, C., Findlay, J. B. C., Zagalsky, P. F., Finet, S. & Receveur-Brechot, V. (2003). *FEBS Lett.* **544**, 189–193.
Di Mascio, P., Kaiser, S. & Sies, H. (1989). *Arch. Biochem. Biophys.* **274**, 532–538.
Durbeej, B. & Eriksson, L. A. (2003). *Chem. Phys. Lett.* **375**, 30–38.
Gerritsen, V. B. (2002). *Protein Spotlight*, Issue 26. Swiss-Prot/Swiss Institute of Bioinformatics.
Gordon, E. J., Leonard, G. A., McSweeney, S. & Zagalsky, P. F. (2001). *Acta Cryst.* D**57**, 1230–1239.
Harman, D. (1981). *Proc. Natl Acad. Sci. USA*, **78**, 7124–7128.
Holden, H. M., Rypniewski, W. R., Law, J. H. & Rayment, I. (1987). *EMBO J.* **6**,1565–1570.
Huber, R., Schneider, M., Epp, O., Mayr,I., Messerschmidt, A., Pflugrath, J. & Kayser, H. (1987). *J. Mol. Biol.* **195**, 423–434.
Huber, R., Schneider, M., Epp, O., Mayr, I., Muller, R., Deutzmann, R., Suter, F., Zuber, H., Falk, H. & Kayser, H. (1987). *J. Mol. Biol.* **98**, 499–513.
Keen, J. N., Caceres, I., Eliopoulos, E. E., Zagalsky, P. F. & Findlay, J. B. C. (1991*a*). *Eur. J. Biochem.* **197**, 407–417.
Keen, J. N., Caceres, I., Eliopoulos, E. E., Zagalsky, P. F. & Findlay, J. B. C. (1991*b*). *Eur. J. Biochem.* **202**, 31–40.
Krawczyk, S. & Britton, G. (2001). *Biochim. Biophys. Acta*, **1544**, 301–310.
Kuhn, R. & Kühn, H. (1967). *Eur. J. Biochem.* **2**, 349–360.
Kuhn, R. & Sorensen, N. A. (1938). *Z. Angew. Chem.* **51**, 465–466.
Marnett, L. J. (1987). *Carcinogenesis*, **8**, 1365–1373.
Meyers, S. P. (1994). *Pure Appl. Chem.* **65**, 1069–1076.
Miki, W. (1991). *Pure Appl. Chem.* **63**, 141–146.
Moody, C. S. & Hassan, H. M. (1982). *Proc. Natl Acad. Sci. USA*, **79**, 2855–2859.
Newbigin, M. I. (1897). *J. Physiol.* **21**, 237–257.
Newbigin, M. I. (1898). *Colour in Nature: a Study in Biology*. London: John Murray.
Newcomer, M. E., Jones, T. A., Aqvist, J., Sundelin, J., Eriksson, U.,

Rask, L. & Peterson, P. A. (1984). *EMBO J.* **3**, 1451–1454.
North, A. C. T. (1993). *Biol. Sci. Rev.* **5**, 31–35.
Papiz, M. Z., Sawyer, L., Eliopoulos, E. E., North, A. C. T., Findlay, J. B. C., Sivaprasadarao, R., Jones, T. A. & Newcomer, M. E. (1986).
Quarmby, R., Norden, D. A., Zagalsky, P. F., Ceccaldi, H. J. & Daumas, R. (1977). *Comp. Biochem. Physiol.* **56B**, 55–61.
Salares, V. R., Young, N. M., Bernstein, H. J. & Carey, P. R. (1979). *Biochim. Biophys. Acta*, **576**, 176–191.
Steinberg, D., Parthasarathy, T. E., Carew, T. E., Khoo, J. C. & Witztum, J. L. (1989). *N. Eng. J. Med.* **320**, 915–924.
Sterling, C. (1964). *Acta Cryst.* **17**, 1224.
Torrissen, O. J. & Christiansen, R. (1995). *J. Appl. Ichthyol.* **21**, 225–230.
Verne, J. (1921). *Bull. Soc. Zool. Fr.* **46**, 61–65.
Wald, G., Nathanson, N., Jencks, W. P. & Tarr, E. (1948). *Biol. Bull., Woods Hole (Mass.)*, **95**, 249–250.
Weesie, R. J., Askin, D., Jansen, F. J. H. M., de Groot, H. J. M., Lugtenburg, J. & Britton, G. (1995). *FEBS Lett.* **362**, 34–38.
Weesie, R. J., Merlin, J. C., de Groot, H. J. M., Britton, G., Lugtenburg, J., Jansen, F. J. H. M. & Cornard, J. P. (1999). *Biospectroscopy*, **5**, 358–370.
Weesie, R. J., Merlin, J. C., Lugtenburg, J., Britton, G., Jansen, F. J. H. M. & Cornard, J. P. (1999). *Biospectroscopy*, **5**, 19–33.
Weesie, R. J., Verel, R., Jansen, F. J. H. M., Britton, G., Lugtenburg, J. & de Groot, H. J. M. (1997). *Pure Appl. Chem.* **69**, 2085–2090.
Wright, C. E., Rafferty, J. B., Flower, D. R., Groom, C. R., Findlay, J. B. C., North, A. C. T., Phillips, S. E. V. & Zagalsky, P. F. (1992). *J. Mol. Biol.* **224**, 283–284.
Zagalsky, P. F. (1976). *Pure. Appl. Chem.* **47**, 103–120.
Zagalsky, P. F. (1985). *Methods Enzymol.* **111**, 216–247.
Zagalsky, P. F. (2003). *Acta Cryst.* D**59**, 1529–1531.
Zagalsky, P. F. & Jones, R. (1982). *Comp. Biochem. Physiol.* **71**, 237–242.
Zanotti, G., Berni, R. & Monaco, H. L. (1993). *J. Biol. Chem.* **268**, 10728–10738.